Chem. Eng. Comm. 1987, vol 58, pp. 431–447

Printed in the United States of America

HEAT TRANSFER TO SPHERES AT LOW TO INTERMEDIATE REYNOLDS NUMBERS

BRUCE A. FINLAYSON and JOHN W. OLSON

Department of Chemical Engineering, BF-10
University of Washington
Seattle, Washington 98195

(Received January 21, 1987; in final form March 20, 1987)

The Navier-Stokes equation and the energy equation are solved using the Galerkin finite element method for flow past a solid sphere at low to intermediate Reynolds numbers. The calculated results are compared with exact theories valid for small or large Peclet numbers. A correlation is provided to predict the numerical results for ranges of Prandtl number from 0.001 to 1000 and Reynolds numbers from 1 to 100. A new correlation is proposed that matches the theoretical results at low Peclet numbers, the numerical results at intermediate Peclet numbers, and the existing experimental data at intermediate to high Peclet numbers.
KEYWORDS Heat transfer Sphere Peclet number

1. INTRODUCTION

Predicting the heat transfer rate between a sphere and a fluid in laminar flow past it is an important problem in multi-phase engineering. When the physical properties are constant, the flow remains laminar for Reynolds numbers up to 130 [Van Dyke, 1982]. Correlations based on experimental data are usually limited to data taken with a few fluids, such as air (Prandtl number = 0.7), water ($Pr = 7$), and oils ($Pr = 200$–higher). Most measurements, however, have been made at Reynolds numbers above 10, as indicated in Figure 1 when the fluid is air.

The two correlations shown in Figure 1 are due to Whitaker [1972] and Vliet and Leppert [1961].

$$Nu = 2 + [0.4\,Re^{1/2} + 0.06\,Re^{2/3}]Pr^{0.4} \tag{1}$$

$$Nu = [1.2 + 0.53\,Re^{0.53}]Pr^{0.3} \tag{2}$$

They differ widely (50–100%) at low Reynolds numbers, and in fact are heavily weighted by data at higher Reynolds numbers (greater than 130) where vortices are shed from the sphere. Thus it would be desirable to have better information for low to intermediate Reynolds numbers.

The Nusselt number is plotted versus Reynolds number with Prandtl number as a parameter in Figure 2, along with Whitaker's correlation. The goal is to predict this variation with Reynolds number and Prandtl number, which is done here in a reasonable fashion. Note, however, that the Reynolds number is seldom as low as 1.0, and the Peclet number (Reynolds number times Prandtl number) is below 1.0

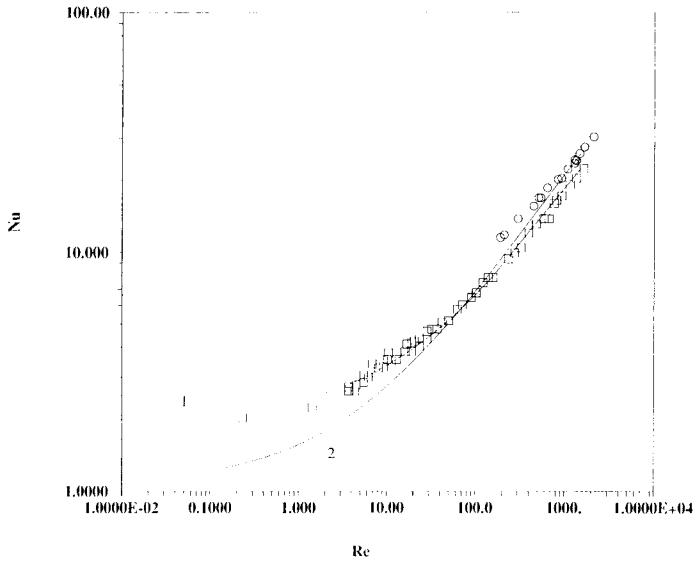

FIGURE 1 Experimental data for air compared with correlations. □ Yuge [1960], ○ Kramers [1946], 1—Whitaker [1972], 2—Vliet and Leppert [1961].

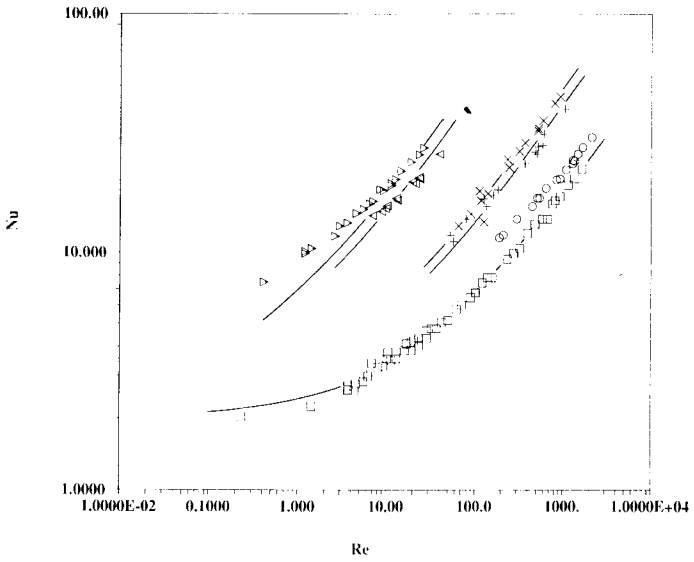

FIGURE 2 Experimental data for air, water, and oil. □ Yuge [1960]; Kramers [1946]: ○ air ($Pr = 0.71$), water ($+$ $Pr = 7.3$; $\times$ $Pr = 10.7$), oil $\triangleleft$ $Pr = 213$, $\triangleright$ $Pr = 380$); —— Whitaker [1972], same Prandtl numbers.

for only one data point. Thus these data cannot be compared with the theoretical results for flow past spheres at low Reynolds numbers and low Peclet numbers.

When the Reynolds number is low, Acrivos and Taylor [1962] derived the following formula for the Nusselt number by solving the heat transfer problem using asymptotic expansions when the flow field was given by Stokes flow.

$$Nu = 2 + \frac{Pe}{2} + \tfrac{1}{4}\, Pe^2 \ln Pe + 0.03404\, Pe^2 + \tfrac{1}{16}\, Pe^3 \ln Pe \quad (Pe < 1,\ Re \to 0)) \quad (3)$$

This expression is only valid as the Peclet number approaches zero. How close to zero one must be is not always clear, although one can make educated guesses by examining the relative importance of first and second order terms. The Peclet number is always less than one, however. When the Peclet number is large, the expression is [Levich, 1959; Friedlander, 1961]

$$Nu = 0.991\, Pe^{1/3} \quad (Pe \to \infty,\ Re \to 0) \quad (4)$$

The size of Peclet number which is sufficiently large to constitute infinity is also not known precisely. Note, however, that the existing correlations do not agree with these limiting behavior. Thus there must be a region of transition between the range of experimental data and the range of these theoretical results. The goal of the numerical work described in this paper is to delineate that transition.

Work recently reported by Chang and one of the authors [1987a, b] considered this same problem for flow past a cylinder. When the physical properties were constant, they solved the flow problem for Prandtl numbers from 0.0073 to 1000 and Reynolds numbers from 0.01 to 50 (where the shedding of vortices begins for flow past a cylinder). These numerical results were then correlated with an expression, whose results compared well with experiments in air. They then did experiments for a Dow Corning fluid when the cylinder was being cooled and the viscosity varied significantly. They did simulations of that case, too, and derived a correlation from the numerical results which agreed well with the experiments. The final correlation was as good as, but no better than, the one due to Zhukauskas [1972] (for experimental data), but Chang's correlation covered a wider range of Prandtl and Reynolds numbers.

Recently Cliffe and Lever [1986] have solved the flow problem numerically for low to intermediate Reynolds numbers, 1 to 100. Their results are probably the most accurate calculations in the literature and they compare them with earlier accurate calculations due to Hamielec *et al.*, [1967], Le Clair, *et al.* [1970], and Dennis and Walker [1971]. For the heat transfer problem with constant physical properties Dennis *et al.* [1973] solved the problem for Reynolds numbers up to 20 and Woo and Hamielec [1971] considered Reynolds numbers up to 300. The problem with variable fluid properties is also important and has been considered recently by Sayegh and Gauvin [1979] and Renksizbulut and Yuen [1983].

In this paper we first report the results of numerical calculations for flow past a solid sphere at Reynolds numbers between 1 and 100 when the fluid has Prandtl numbers from 0.001 to 1000 and the physical properties are constant. We then provide a correlation of the numerical data that covers the wide range of

parameters. The correlation itself has some interesting twists that are only revealed through the numerical calculations. The correlation is compared with experimental results in the literature for air, water and oil. Finally additional solution details are provided that illustrate the temperature contours in the region of parameter space where the correlation provides a transition from the low Peclet to the high Peclet region. The additional complication of variable physical properties is left to future work.

2. NUMERICAL CALCULATIONS

The heat transfer problem is formulated as steady, laminar flow in two dimensions for a Newtonian fluid. All physical properties are taken as constant. The momentum equation is solved in dimensionless form

$$Re\,\mathbf{u}\cdot\nabla\mathbf{u} = -\nabla p + \nabla\cdot[\nabla\mathbf{u} + \nabla\mathbf{u}^T] \tag{5}$$

along with the continuity equation

$$\nabla\cdot\mathbf{u} = 0 \tag{6}$$

and the energy equation

$$Pe\,\mathbf{u}\cdot\nabla T = \nabla^2 T \tag{7}$$

The equations are solved using the Galerkin finite element method [Finlayson, 1980]. In this version of the Method of Weighted Residuals, each equation is multiplied by a weighting function, certain terms in the equation are integrated by parts and the boundary conditions are applied. The resulting equations are non-linear and are solved by first linearizing them in order to apply the Newton–Raphson iterative method. The resulting equations are

$$-\int_V \delta p\,\nabla\cdot\mathbf{u}^{s+1}\,dV = 0 \tag{8}$$

$$\int_V \nabla\delta\mathbf{u}:(\nabla\mathbf{u}^{s+1} + \nabla\mathbf{u}^{T,s+1})\,dV - \int_V p^{s+1}\nabla\cdot\delta\mathbf{u}\,dV - \int_V \delta\mathbf{u}\cdot\mathbf{f}\,dV + Re\int_V \delta\mathbf{u}\cdot(\mathbf{u}^s\cdot\nabla\mathbf{u}^{s+1} + \mathbf{u}^{s+1}\cdot\nabla\mathbf{u}^s - \mathbf{u}^s\cdot\nabla\mathbf{u}^s)\,dV = 0 \tag{9}$$

$$\int_V \delta T\,Pe(\mathbf{u}^s\cdot\nabla T^{s+1} + \mathbf{u}^{s+1}\cdot\nabla T^s - \mathbf{u}^s\cdot\nabla T^s)\,dV + \int_V \nabla\delta T\cdot\nabla T^{s+1}\,dV + \int_S \delta T\,\mathbf{n}\cdot\mathbf{q}\,dS = 0 \tag{10}$$

The terms $\mathbf{f}$ and $\mathbf{q}$ represent applied surface traction and heat flux. The finite element approximation used is biquadratic elements for velocity and temperature and bilinear elements for pressure. The elements are isoparametric and irregular elements are transformed into rectangles to calculate the integrals arising from the Galerkin method. The frontal routine [Hood, 1976] was used to perform the

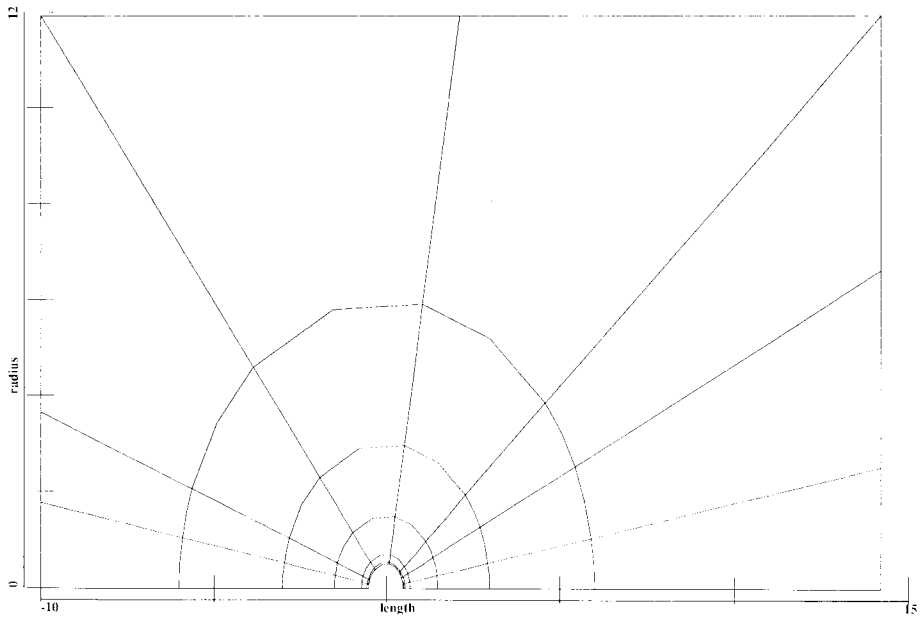

FIGURE 3 Finite element mesh.

LU decomposition of the final matrix. The computer program is called VEHEAT, and also has capability for variable viscosity and viscoelastic fluids [Finlayson and McClelland, 1985].

A typical flow geometry and finite element mesh is illustrated in Figure 3. The problem is solved in cylindrical coordinates; this means that the top surface is a tube. Along the surface of the sphere the velocity components u and v are taken as zero; the temperature is 1.0. At the entrance to the left the velocity is uniform, $u = 1$, $v = 0$, and the temperature is zero. The mesh must extend sufficiently far upstream to insure that fully developed conditions are appropriate there, and this is checked *a posteriori.* Along the centerline the transverse velocity is taken as zero and natural boundary conditions are used for axial velocity and temperature: no applied axial force or normal heat flux. At the top surface the boundary condition is taken as no applied forces or heat flux. Due to the use of natural boundary conditions, and the fact that the Galerkin equations provide an integrated differential equation, the solution is appropriate to the case of an infinite fluid. Neither $u = 1$, nor $v = 0$, nor $T = 0$ will necessarily be obtained there, nor are they required there. If we had wanted to see the effect of a solid or slip tube different boundary conditions would have been necessary. The downstream boundary condition is also a natural boundary condition; this permits the solution of the problem on a domain that is shorter than needed to achieve fully-developed flow downstream.

A critical part of applying the Galerkin method is to design a mesh that is both economical and sufficient for the problem at hand. In order to resolve the thin

thermal boundary layer at the frontal stagnation point, small elements are used there; similarily small elements are needed behind the cylinder, too, since separation occurs and reverse flow is expected for intermediate Reynolds numbers. The relative radial sizes of the elements are 0.04, 0.16, 0.80, 1.5, 3.0, 4.0 (for the leading edge) or 8.2 (for the trailing edge). These sizes are all measured with respect to the diameter of the cylinder. An effort was made to keep the cell Peclet number and cell Reynolds number less than 2.0, to avoid oscillations in the solution [Jensen and Finlayson, 1980].

$$Re_{\text{cell}} = Re\frac{|u|\,\Delta x}{2Ud}, \qquad Pe_{\text{cell}} = Pe\frac{|u|\,\Delta x}{2Ud} \tag{11}$$

While the cell Reynolds or Peclet defined in terms of the upstream velocity may be greater than 2.0 ($Pe = 1000$, $\Delta r = 0.04$, $Pe_{\text{cell}} = 40$), the velocity is low in the region of the sphere (where the gradient is large enough to cause oscillations) and the complete cell Reynolds number and Peclet number is near 2. The spherical surface is modeled exactly by the quadratic isoparametric elements with angular element sizes of 10, 10, 30, 50, 40, 15, 15, and 10 degrees.

This mesh was examined in a detailed fashion by Chang and Finlayson [1987] for problem of flow past a cylinder and found to be quite adequate. Energy balances averaged 4 per cent over key regions of the flow. Comparing with the calculations of Cliffe and Lever [1986] shows that they use an inner element size of 0.043 (based on the sphere diameter), whereas we use a value of 0.04. Our calculations for the drag coefficient agree with theirs within 3% on the average.

The heat transfer coefficient is defined as

$$Nu_\phi = -2\left.\frac{\partial T}{\partial r}\right|_{r=R} \tag{12}$$

The factor of 2 comes from using the diameter of the sphere as the characteristic distance. To evaluate the derivative, the following difference formula was used, based on the quadratic approximation of temperature.

$$Nu = \frac{2(3\theta_1 - 4\theta_2 + \theta_3)}{\Delta r} \tag{13}$$

The θ_1, θ_2, and θ_3 are the temperatures at the wall, $\Delta r/2$, and Δr, respectively. The mean Nusselt number is defined as

$$Nu = \frac{1}{\pi}\int_0^\pi Nu_\phi \, d\phi \tag{14}$$

and is calculated by quadratic interpolation.

$$Nu = \frac{1}{\pi}\sum_I \Delta\phi_I\left(\tfrac{1}{6}\,Nu_{\phi 1} + \tfrac{2}{3}\,Nu_{\phi 2} + \tfrac{1}{6}\,Nu_{\phi 3}\right)_I \tag{15}$$

Here $\Delta\phi_I$ is the I-th azimuthal step size and $Nu_{\phi i}$ are the local Nusselt numbers at the nodes 1,,2 and 3 in the I-th element.

The results of the simulations are listed in Table I. The Nusselt numbers for

TABLE I

Numerical results

Re	*Pe*	*Pr*	*Nu*
1	0.2	0.2	2.087
	0.5	0.5	2.205
	0.73	0.73	2.273
	1.0	1.0	2.341
	2.0	2.0	2.543
	5.0	5.0	2.943
	7.3	7.3	3.161
	10.0	10.0	3.373
	100.0	100.0	6.083
	1000.0	1000.0	11.03
10	0.2	0.02	2.092
	0.5	0.05	2.224
	1.0	0.10	2.386
	2.0	0.20	2.632
	5.0	0.50	3.118
	10.0	1.0	3.642
	100.0	10.0	6.729
	1000.0	100.0	12.83
100	0.2	0.002	2.094
	0.5	0.005	2.234
	1.0	0.01	2.416
	2.0	0.02	2.708
	5.0	0.05	3.323
	10.0	0.10	4.015
	100.0	1.0	7.953
	1000.0	10.0	16.74

Peclet numbers of 0.01 and smaller were slightly less than 2 (averaging 1.3% less). Since these results are contrary to theory they are excluded, even though the errors are small and presumably due to numerical error. Values of Peclet of 0.01 and 0.1 were thus excluded. To assess the accuracy of the other calculations they are compared with literature values in Table II. The values of drag coefficient are compared with those of Cliffe and Lever [1986], who made a detailed comparison of finite element methods and compared prior results as well. The drag coefficients agree with a mean square error of 4%. The Nusselt numbers are compared with those of Dennis *et al.* [1973] and Woo and Hamielec [1971] and agree with a mean square error of 1%. Based on these comparisons we have confidence in the results for the same parameter ranges.

The next comparison is between the numerical results and the theoretical results, valid for low Reynolds number and low Peclet number. To accentuate the comparison we plot $Nu - 2$ versus Prandtl number in Figure 4, for Reynolds numbers of 1, 10, and 100. It is clear that the curves for different Reynolds number have similar shapes so that whatever correlation applies at low Reynolds number (where the theory applies) can be used at higher Reynolds number, too. If the heat transfer problem just depended on Peclet number, as is the case for low Reynolds number, then the adjacent points would have the same value of

TABLE II

Comparison with literature

Re	*Drag coefficient* This report	Cliffe and Lever [1986]
1	27.76	27.16
5	7.238	7.033
10	4.390	4.259
30	2.196	2.122
50	1.646	1.574
70	1.376	1.309
100	1.145	1.087

Re	*Nusselt number* This report ($Pr = 0.73$)	Dennis *et al.* [1973] ($Pr = 0.73$)	Woo and Hamielec [1971] ($Pr = 0.71$)
0.1	1.997	2.037	2.028
0.2	2.052	2.064	2.058
0.5	2.156	2.151	2.136
1.0	2.273	2.260	2.246
2.0	2.459		2.430
5.0	2.877	2.857	2.843
10.0	3.384	3.358	3.34

$Nu - 2$. This is nearly the case for low Peclet number ($Pe = 0.2$). This suggests that the low Peclet number theory can be applied safely up to $Pe = 0.2$, even for Reynolds numbers as high as 100. The low Peclet number theory was of course obtained using the flow field appropriate to $Re = 0$. Acrivos and Taylor [1962] and Rimmer [1968] also showed that the low and high Peclet number theory was

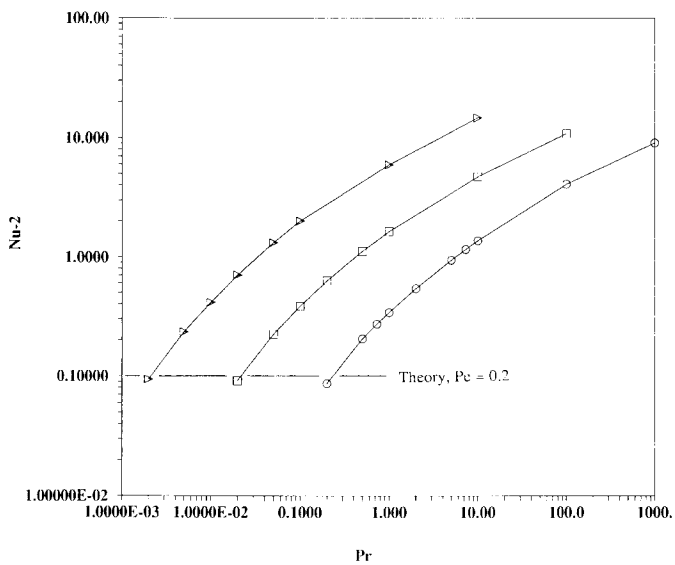

FIGURE 4 Numerical results for $Nu - 2$. ○ $Re = 1$, □ $Re = 10$, △ $Re = 100$.

TABLE III

Accuracy of correlations for predicting numerical data

Source	Eq.	Mean square error	Correlation coeff.
Whitaker [1972]	1	10.4%	0.9962
Vliet and Leppert [1961]	2	26.4%	0.9805
This work	18	1.6%	0.9994
This work	20	6.5%	0.9975

influenced only slightly by Reynolds number, for small $Re < 1$. These results suggest this holds for Reynolds numbers as large as 100. This result in itself shows the power of numerical calculations to extend the range of validity of asymptotic results. Notice at high Prandtl number (corresponding to high Peclet number) that the curves approach a straight line on this log-log graph. The slope for the last two data points and different Reynolds numbers is 0.258 for $Re = 1$, 0.280 for $Re = 10$, and 0.328 for $Re = 100$. These numerical results also approach the high Peclet number asymptotes, and these asymptotes seem to have the same form, although they are reached for lower Prandtl numbers when the Reynolds number is larger. Again, the theoretical results for low Reynolds number seem to hold at much higher Reynolds number, although the coefficients in the correlation would vary. The final point to be learned from Figure 4 is that a correlation based on dependence of Prandtl number to a power will be unsuccessful in corrleating these results, since a straight line does not fit the curves in Figure 4. The value of $Nu - 2$ requires Prandtl number to a power of 1.0 at low Prandtl number (low Peclet number) and 1/3 at high Prandtl number (high Peclet number).

3. CORRELATION OF NUMERICAL RESULTS

It is desirable to use the numerical results to determine the form of the best correlation of Nusselt number as a function of Reynolds number and Prandtl number. Since we can do simulations for whatever parameters we want, we can provide detailed cross-plots which help identify the correct form of correlation. We want the correlation to obey

$$Nu = 2 + \frac{Pe}{2} \quad (Pe \to 0,\ Re \to 0) \tag{16}$$

since that expression is satisfied for all $Pe < 0.1$, even for Reynolds number as large as 100. For high Peclet number we want the correlation to reduce to Eq. (4), with some adjustment at different Reynolds numbers. The following combination is suggested in the mass transfer studies by Zhang and Davis [1987] using the idea of Churchill and Usagi [1972].

$$\frac{1}{(Nu-2)^n} = \frac{1}{(Pe/2)^n} + \frac{1}{(c\, Pe^{1/3}\, Re^m)^n} \tag{17}$$

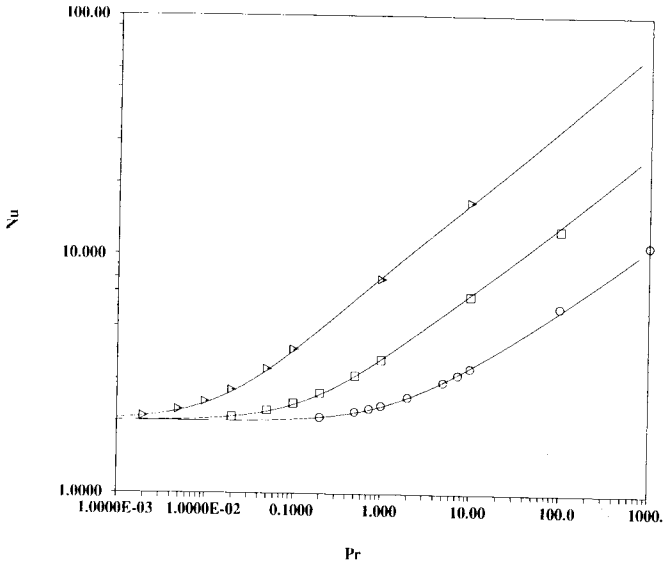

FIGURE 5 Correlation of numerical data with Eq. (18). ○ $Re = 1$, □ $Re = 10$, △ $Re = 100$.

The parameters c, m, and n were determined by minimizing the mean square error between the predictions of Eq. (17) and the numerical data. The best results were with $c = 0.9$, $m = 0.11$, and $n = 1.0$, giving a mean square error of 1.6%. Thus the best correlation of the numerical data is

$$\frac{1}{(Nu-2)} = \frac{1}{(Pe/2)} + \frac{1}{(0.9\,Pe^{1/3}\,Re^{0.11})} \tag{18}$$

Comparison of this equation with the numerical results is displayed in Figure 5 and is excellent.

Another alternative was to use the Whitaker correlation (2) in a similar way. Eq. (2) is first expressed in terms of Peclet number and Reynolds number rather than Prandtl number and Reynolds number, since the major effect seen in Figure 4 is the Peclet number rather than the Prandtl number).

$$Nu = 2 + 0.4\,Pe^{0.4}\,Re^{0.1} + 0.06\,Pe^{0.4}\,Re^{0.27} \tag{19}$$

The correlation was tried in the form

$$\frac{1}{(Nu-2)^n} = \frac{1}{(Pe/2)^n} + \frac{1}{(0.4\,Pe^{0.4}\,Re^{0.1} + 0.06\,Pe^{0.4}\,Re^{0.27})^n} \tag{20}$$

The best value of n was 2.4, giving a mean square error of 6.5% when predicting the numerical results. The comparison of this equation with the numerical results is displayed in Figure 6 and is not as good as that obtained by Eq. (18) as shown in Figure 5.

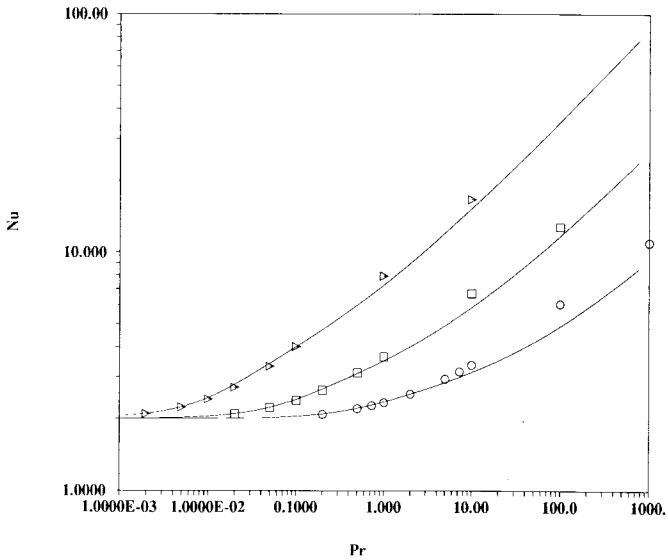

FIGURE 6 Correlation of numerical data with Eq. (20). ○ $Re = 1$, □ $Re = 10$, △ $Re = 100$.

Based on these results, the best correlation of the numerical results is Eq. (18). The underpinnings for this form are the asymptotic theory for low Peclet number and zero Reynolds number, and the numerical results for the range of Reynolds number between 1 and 100, and Prandtl number between 0.002 and 1000, and Peclet number between 0.2 and 1000.

4. COMPARISON WITH EXPERIMENT

The new correlation, Eq. (18), is compared with experimental data for air in Figure 7. This figure can be compared with Figure 1 which shows the comparison with existing correlations, Whitaker's existing correlation, Eq. (1), and Eq. (18) do an adequate job. The major difference is that Eq. (18) is slightly closer to the data for the two data points at the lowest Reynolds numbers. Vliet and Leppert's correlation, Eq. (2), is adequate for the air data but is clearly wrong at low Peclet number. The mean square errors are listed in Table IV. Eq. (1) has a mean square error of 9.9%, whereas Eq. (18) has a mean square error of 9.7%, a slight improvement.

The next test of the correlation is whther it can adequately handle the change of Nusselt number when the fluid has a higher Prandtl number. For this reason we use the data for air, water and oil, with data from Yuge [1960] and Kramers [1946]. The new correlation, Eq. (18) is compared with the data in Figure 8. The two data points at low Reynolds number for air are the only data points with $Pe \leq 1$, and the numerical results model them adequately. [The error bars in

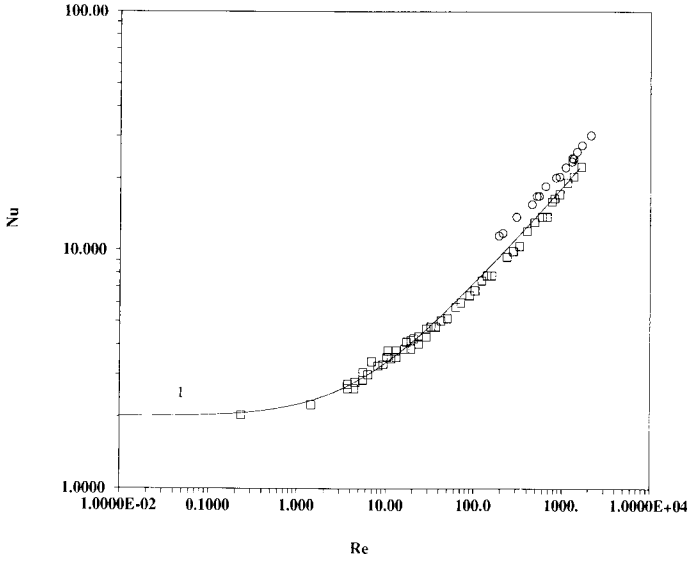

FIGURE 7 Experimental data for air correlated with Eq. (18). □ Yuge [1960], ○ Kramers [1946], 1—Eq. (18).

Yuge are large enough to encompass the numerical results.] The mean square error of the two correlations is given in Table V. Eq. (1) and (2) have mean square errors of 10.4%. These correlations were chosen to fit the experimental data. Eq. (18) has a mean square error of 9.4% (for the experimental results) and was chosen to fit the numerical results. Yet it represents the experimental data slightly better than the other correlations. The Vliet and Leppert [1961] correlation (2) is clearly inadequate at low Peclet number. Whitaker's correlation [1972] (2) is good for predicting the Nusselt number, but is less good for predicting $Nu - 2$ at low Peclet numbers (see line 4 in Figure 8). Eq. (18) agrees with theory at low Peclet number, predicts $Nu - 2$ well for intermediate Peclet numbers, and predicts the experimental data for intermediate to large Peclet number.

TABLE IV

Accuracy of Correlations for Predicting Experimental Data for Air

Source	Eq.	Mean square error	Correlation coeff.
Whitaker [1972]	1	9.9%	0.9869
Vliet and Leppert [1961]	2	15.6%	0.9870
This work	18	9.4%	0.9855
This work	20	9.7%	0.9869

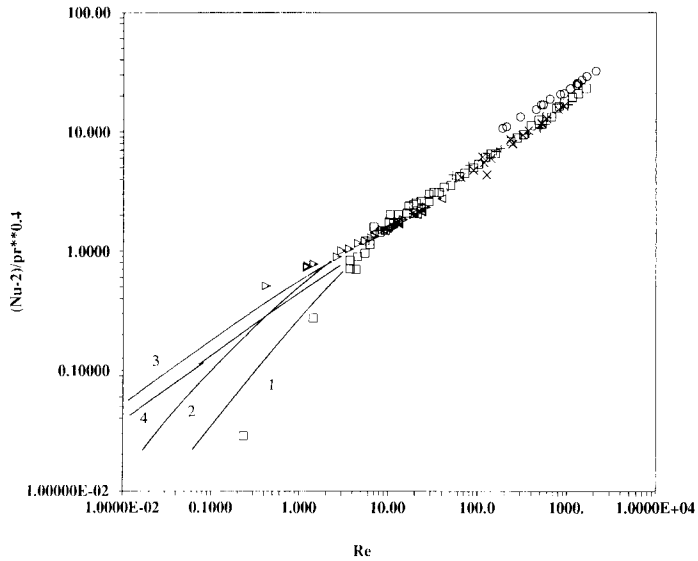

FIGURE 8 Experimental data for air, water and oil as correlated with Eq. (1) and Eq. (18). Symbols are the same as in Figure 2. The lines are for Eq. (18): 1—$Pr = 0.71$, 2—$Pr = 7.3$, 3—$Pr = 380$, 4—Eq. (1).

TABLE V

Accuracy of correlations for predicting experimental data

Source	Eq.	Mean square error	Correlation coeff.
Water (*Prandtl number* = 7.3 *and* 10.7)			
Whitaker [1972]	1	12.0%	0.9945
Vliet and Leppert [1961]	2	5.4%	0.9953
This work	18	9.1%	0.9941
This work	20	12.1%	0.9945
Oil (*Prandtl number* = 213 *and* 380)			
Whitaker [1972]	1	9.9%	0.9903
Vliet and Leppert [1961]	2	8.5%	0.9877
This work	18	9.5%	0.9876
This work	20	10.2%	0.9903
All Data (*Prandtl number* = 0.714, 7.3, 10.7, 213, 380)			
Whitaker [1972]	1	10.4%	0.9872
Vliet and Leppert [1961]	2	10.4%	0.9908
This work	18	9.4%	0.9837
This work	20	10.4%	0.9849

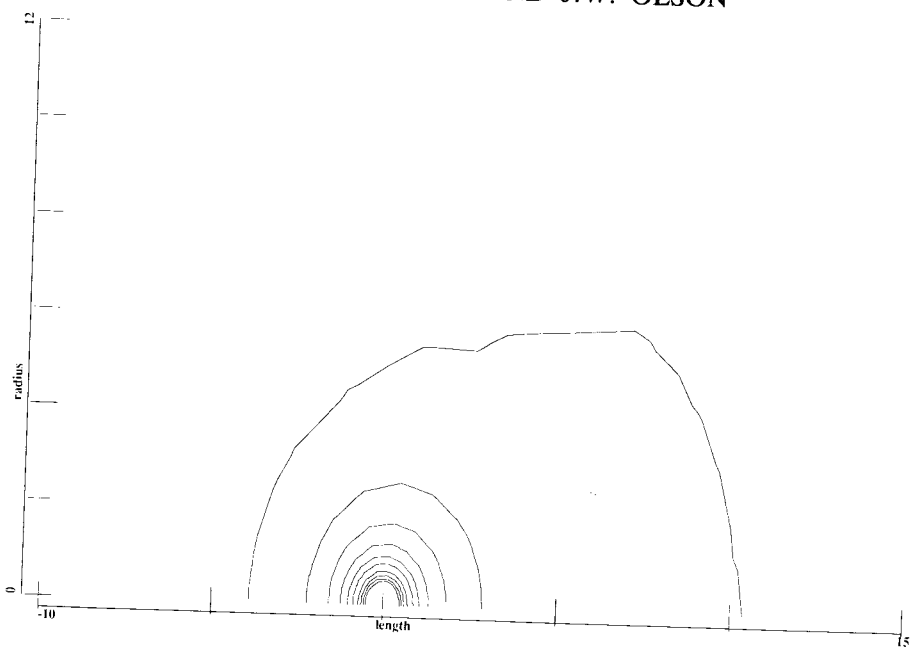

FIGURE 9 Temperature contours, $Pe = 0.1$, $Re = 1$, Contour levels are 0.1 (0.1) 1.0.

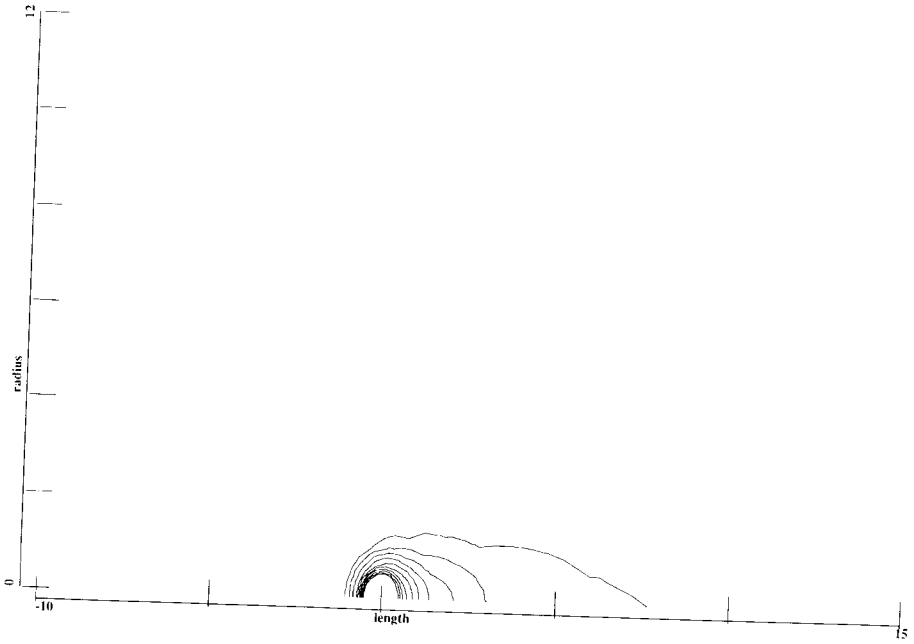

FIGURE 10 Temperature contours, $Pe = 10$, $Re = 1$. Contour levels are 0.1 (0.1) 1.0.

5. SOLUTION DETAILS

Figure 9 gives the temperature contours for the case $Pe = 0.1$, $Re = 1$. Contours were also drawn for other Reynolds (10 and 100), but these are almost identical. Even though the streamlines are widely different (some cases show recirculation, some do not), there is little effect on the heat transfer when the Peclet number is so low. If one keeps the Reynolds number fixed and increases the Prandtl number (thus increasing the Peclet number), then there is an effect in the contours, as shown in Figure 10. [Note that the slight wiggles in the contour plots are partially due to the straight line approximations used in the interpolation routines.] For this problem the Peclet number is clearly the major variable; Reynolds number variations, keeping Peclet number fixed, has little effect. This conclusion agrees with the theoretical results of Acrivos and Taylor [1962] and Rimmer [1968] at low Reynolds numbers.

6. CONCLUSIONS

The numerical results showed that the theoretical formulas Eq. (3–4), derived for low Reynolds number, are in fact valid for higher Reynolds number, including the range 1 to 100; the high Peclet number asymptote must be adjusted with a slight dependence on Reynolds number. The numerical results also showed that the existing empirical correlations are not valid outside the range of data for which there were derived. The best correlation of both numerical results and experimental data is Eq. (18). This equation is based on fitting the asymptotic theory and numerical results alone, in the range $Pr = 0.002$ to 1000, $Re = 1$ to 100, and $Pe = 0.2$ to 1000. It also does the best job in predicting the experimental results, with no adjustment of parameters, in the range $Pr = 0.71$, $Re = 0.2$ to 2100, and $Pe = 0.16$ to 10,000. While this result may be fortuitous, the results clearly show the value of the numerical calculations in the stated range.

NOMENCLATURE

C_p	heat capacity
d	diameter of sphere
$\mathbf{f}$	body force
k	thermal conductivity
p	pressure
δp	pressure weighting function in Galerkin method
$\mathbf{q}$	heat flux
Nu	Nusselt number, defined by Eq. (12, 15)
Pe	Peclet number, $\rho C_p U d/k$

Pr Prandtl number, $C_p\mu/k$

Re Reynolds number, $\rho Ud/\mu$

S surface area

T temperature

δT temperature weighting function in Galerkin method

$\mathbf{u}$ velocity

$\delta\mathbf{u}$ velocity weighting function in Galerkin method

U upstream velocity

V volume

Superscripts and subscripts

s iteration number

ϕ function of angle ϕ

Greek letters

ρ density

μ viscosity

ϕ angular position

REFERENCES

Acrivos, A., and Taylor, T.D., "Heat and Mass Transfer from Single Spheres in Stokes Flow", *Physics Fluids* **5,** 387–394 (1962).

Chang, M.W., and Finlayson, B.A. "Heat Transfer in Flow Past Cylinders. Part I. Calculations for Constant Fluid Properties," *Numerical Heat Transfer* **12** (1987).

Chang, M.W., Sleicher, C.A., and Finlayson, B.A., "Heat Transfer in Flow Past Cylinders at $Re < 150$. Part II. Experiments and Theory for Variable Fluid Properties." *Numerical Heat Transfer* **12** (1987).

Churchill, S.W., and Usagi, R., "A General Expression for the Correlation of Rates of Transfer and other Phenomena," *A.I.Ch.E.J.* **18,** 1121–1128 (1972).

Cliffe, K.A., and Lever, D.A., "A Comparison of Finite-Element Methods for Solving Flow Past a Sphere," *J. Comp. Phys.* **62,** 321–330 (1986).

Dennis, S.C.R., and Walker, J.D.A., "Calculation of the Steady Flow Past a Sphere at Low and Moderate Reynolds Numbers," *J. Fluid Mech.* **48,** 771–789 (1971).

Dennis, S.C.R., Walker, J.D.A., and Hudson, J.D., "Heat Transfer from a Sphere at Low Reynolds Numbers," *J. Fluid Mech.* **60,** 273–283 (1973).

Finlayson, B.A., *Nonlinear Analysis in Chemical Engineering,* McGraw-Hill (1980).

Finlayson, B.A., and McClelland, M.A., "Non-isothermal Extrudate Swell of Elastic Fluids," pp. 269–287 in *Numerical Methods in Heat Transfer, Vol. III* (Ed. R.W. Lewis and K. Morgan, Pineridge Press) (1985).

Friedlander, S.K., "A Note on Transport to Spheres in Stokes Flow," *A.I.Ch.E.J.* **7,** 347–8 (1961).

Hamielec, A.E., Hoffman, T.W., Ross, L.L., "Numerical Solution of the Navier-Stokes Equation for Flow Past Spheres: Part 1. Viscous Flow Around Spheres with and without Radial Mass Efflux," *A.I.Ch.E.J.* **13,** 212–219 (1967).

Hood, P., "Frontal Solution Program for Unsymmetric Matrices," *Int. J. Num. Methods Eng.* **10,** 379–399 (1976).

Jensen, O.K., and Finlayson, B.A., "Oscillation Limits for Weighted Residual Methods," *Int. J. Num. Methods Eng.* **15,** 1681–1689 (1980).

Kramers, H., "Heat Transfer from Spheres to Flowing Media," *Physica* **12,** 61–80 (1946).

Le Clair, B.P., Hamielec, A.E., and Pruppacher, H.R., "A Numerical Study of the Drag on a Sphere at Low and Intermediate Reynolds Numbers," *J. Atmos. Sci.* **27,** 308–315 (1970).

Levich, V.G., *Physicochemical Hydrodynamics,* Moscow (1959).

Renksizbulut, M., and Yuen, M.C., "Numerical Study of Droplet Evaporation in a High-Temperature Stream," *Trans. ASME, J. Heat Transfer,* **105,** 389–396 (1983).

Rimmer, P.L., "Heat Transfer from a Sphere in a Stream of Small Reynolds Number," *J. Fluid Mech.* **32,** 1–8 (1968).

Sayegh, N.N., and Gauvin, W.H., "Numerical Analysis of Variable Property Heat Transfer to a Single Sphere in High Temperature Surrounding," *A.I.Ch.E.J.* **25,** 522–534 (1979).

Van Dyke, M., *An Album of Fluid Motion,* Parabolic Press, p. 33 (1982).

Vliet, G.C., and Leppert, G., "Forced Convection Heat Transfer From an Isothermal Sphere to Water," *Trans. ASME, J. Heat Transfer* **83,** 163–175 (1961).

Whitaker, S., "Forced Convection Heat Transfer Correlations for Flow in Pipes, Past Flat Plates, Single Cylinders, Single Spheres, and for Flow in Packed Beds and Tube Bundles," *A.I.Ch.E.J.* **18,** 361–371 (1972).

Woo, S.E., and Hamielec, A.E., "A Numerical Method of Determining the Rate of Evaporation of Small Water Drops Falling at Terminal Velocity in Air," *J.Atmos. Sci.* **28,** 1448–1454 (1971).

Yuge, T., "Experiments on Heat Transfer From Spheres Including Combined Natural and Forced Convection," *Trans. ASME, J. Heat Transfer* **82,** 214–220 (1960).

Zhang, S.H., and Davis, E.J., "Mass Transfer from a Single Micro-droplet to a Gas Flowing at Low Reynolds Number," *Chem. Eng. Comm.* **50,** 51–68 (1987).

Zhukauskas, A.A., "Heat Transfer of Tubes in Crossflow," *Adv. Heat Trans.* **8,** 93–160 (1972).